URSI GASS 2020, Rome, Italy, 29 August - 5 September 2020

ITALSAT Ka, Q and V band Cross Polar Discrimination Statistics Measured in Pomezia, Italy

Eric Regonesi*(1), Antonio Martellucci(2), Carlo Riva(1)(3) and Lorenzo Luini(1)(3)
(1) DEIB: Politecnico di Milano, Milan, Italy, eric.regonesi@polimi.it
(2) European Space Agency (ESA), Noordwijk, The Netherlands
(3) IEIIT: Consiglio Nazionale delle Ricerche (CNR), Milan, Italy

Abstract

The availability of reliable measurements on atmospheric depolarization is fundamental for the improvement of the current Cross Polar Discrimination (XPD) prediction models. In particular, the joint rain attenuation and XPD statistics are foreseen to be the basis in this process. The statistical analysis presented in this contribution for the site of Pomezia (Rome), within the scope of the Italsat experiment, provides the reference information for the development of models at Ka, Q and V bands.

1 Introduction

New generation satellite communication (SatCom) links require an accurate design to fully exploit the potential transfer of data. The interest in Q/V bands is increasing as they are foreseen to be the future of commercial electromagnetic SatCom systems [1]. Furthermore, the dual polarization transmission is a sound technique to maximize the link capacity. As already discussed in literature [2], the atmosphere has a definite impact on the electromagnetic waves, such as Faraday rotation, additional attenuation and phase shift and, for dual polarization systems, the variation of the polarization state. The latter effect comes mainly from the non-sphericity of the hydrometeors present in the troposphere, like raindrops and ice particles. Reliable experiments on such an impairment are hard to be set up. Among them, the ITALSAT campaign started in 1992 came with the aim of assessing the troposphere effect on electromagnetic microwave links at three different bands, Ka, Q and V. The experiment planned three main ground stations in Turin, Spino d'Adda (Milan) and Pomezia (Rome) [3] to record satellite beacons data. This contribution reports the cross polar discrimination (XPD) cumulative statistics of the Pomezia site. The availability of reliable data on the depolarization is the first step towards the improvement of the current XPD prediction models.

2 The cross polar discrimination

The generic effect of an atmospheric slab on the electric field can be expressed by [4]

$$\begin{bmatrix} E_{1,out} \\ E_{2,out} \end{bmatrix} = \begin{bmatrix} T_{11} & T_{12} \\ T_{21} & T_{22} \end{bmatrix} \begin{bmatrix} E_{1,in} \\ E_{2,in} \end{bmatrix}. \quad (1)$$

$E_{1,in}$ and $E_{2,in}$ represent the electric field components of the signal $\mathbf{E}_{in}$ entering the slab. Analogously, the left terms of (1) represent its output electric field $\mathbf{E}_{out}$. The coefficients T_{ij} $(i,j = \{1,2\})$ form the polarization transfer matrix $\mathbf{T}$. The subscripts 1,2 may indicate a generically polarized component. In this contribution, we will refer either to horizontal (H) and vertical (V) polarization in the linear case, or to right-handed (R) and left-handed (L) polarization in the circular case. The first quantity of interest is the complex cross polar ratio (XPR), defined as [4]

$$\delta_{ij} = \frac{T_{ij}}{T_{jj}},\ (i \neq j). \quad (2)$$

The XPR will be useful in the correction of the singular polarization signals. Starting from the XPR, we can extract the cross polar discrimination (XPD) as [4]

$$\mathrm{XPD}_{ij} = 20\log_{10}\left|\delta_{ij}\right|. \quad (3)$$

The XPD expresses quantitatively the cross-talk between two orthogonally polarized signals through the medium. The in-force ITU-R Recommendation P.618-13 [5] provides a method to estimate the XPD starting from the knowledge of the long term statistics of the excess attenuation with respect to clear sky conditions, also known as the co-polar attenuation (CPA). ITU-R P.618 links the not exceeded rain XPD (defined with opposite sign convention with respect to (3)) to the cumulative distribution of CPA. The ice contribution is taken into account by an additional term in decibels, still based on the rain XPD. The need of joint distributions of CPA and XPD is suggested by looking at the predictions given by the model and the recorded data in measurements campaigns (see Figure 19 of [4], for example). In this work we present the cumulative statistics of XPD conditioned to CPA, along with the correspondent prediction by ITU-R P.618.

3 Dataset

The dataset is a collection of 66 events recorded at the Pomezia station site in 1994-1999. The events are a depolarization significant subset of the data recorded during the ITALSAT campaign between 1993 and 2000. The ITALSAT satellite was geostationary, at a longitude of 13.2° E [3]. The transmitted beacons were at 18.7, 39.6 and 49.5 GHz. The polarizations of the beacons at the three

frequencies were vertical, right-handed, and horizontal-vertical switched, respectively. The Pomezia ground station (41.7° N, 12.5° E, 108 m a.m.s.l) was equipped with a receiving antenna of 3.5 m diameter, at an elevation angle of 41.8°. The collected data underwent a two-stage processing. Firstly, data were removed of the bias on the depolarization, coming from the transmitting and receiving chains. Secondly, the processed data were used to extract the overall XPD statistics, presented by means of the scatterplot between the XPD and the CPA, and the complementary cumulative distribution function (CCDF) of the XPD itself. The pre-processing stage was slightly different if the transmitted signals had either one or two orthogonal components.

3.1 Single polarization signals at 18.7 and 39.6 GHz

For the linear and circular polarizations at 18.7 and 39.6 GHz, respectively, we extracted separately the CPA and the XPR. The reference clear sky attenuation signal A_{ref} was created by interpolating the average attenuation level in the minutes right before and after the event. The attenuation A_{tot} was extracted from the co-polar signal. We removed the clear sky contribution to A_{tot} by subtraction, to get the excess attenuation A_{exc},

$$A_{exc}(t) = A_{tot}(t) - A_{ref}(t). \quad (4)$$

Then, we filtered it with a $\cos^2$-shaped low pass filter, whose cutoff frequency was set to $f = 0.025$ Hz, to remove the scintillations [6]. The XPR was extracted by (2). The reference XPR was also evaluated by (2), but using as transfer coefficients the time interpolated signals between their average values in the minutes right before and after the event. The correction applied was simply the difference between the measured and the reference XPR [7],

$$\delta_{ij,corr}(t) = \delta_{ij}(t) - \delta_{ij,ref}(t). \quad (5)$$

We applied to the XPR an adaptive low-pass filter, based on the corresponding punctual (in time) level of the XPD. The actual thresholds on the XPD can be found in [4]. The lower (thus, noisier) the XPD, the longer was the moving average window in the time domain. The filter was selected to be $\cos^2$-shaped, with an averaging window ranging from 5 to 60 s.

3.2 Dual polarization signal at 49.5 GHz

The presence of two linear polarizations at 49.5 GHz allowed a matrix correction directly on the polarization transfer coefficients. Similarly to [4], we decided to correct the clear sky effect by a left multiplication, which implied assigning all the system depolarization effects to the ground station,

$$\mathbf{T}_{corr}(t) = \mathbf{T}_{ref}(t)^{-1} \cdot \mathbf{T}(t), \quad (6)$$

where $\mathbf{T}_{ref}(t)$ is the linearly interpolated polarization transfer matrix between its averaged values in the few minutes before and after the event. The outcoming transfer matrix entered an adaptive low-pass filter, as did for the XPR in 3.1. The XPD was finally calculated through (2) and (3).

4 Cross Polar Discrimination statistics

4.1 XPD statistics analysis at Ka band

In Figure 1 we reported the XPD and CPA scatterplot of the linearly polarized beacon at 18.7 GHz. As reference, we

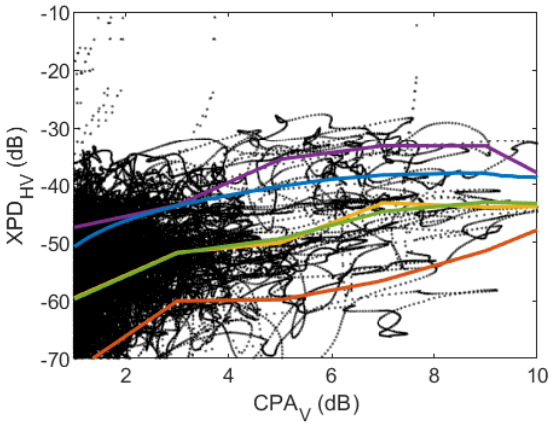

Figure 1. Scatterplot of XPD_{HV} and CPA_V, at 18.7 GHz. Red, yellow and purple curves are the 10, 50 and 90 percentiles of XPD conditioned to CPA values. The green curve is the mean. The cyan curve is the ITU-R P.618-13 model prediction.

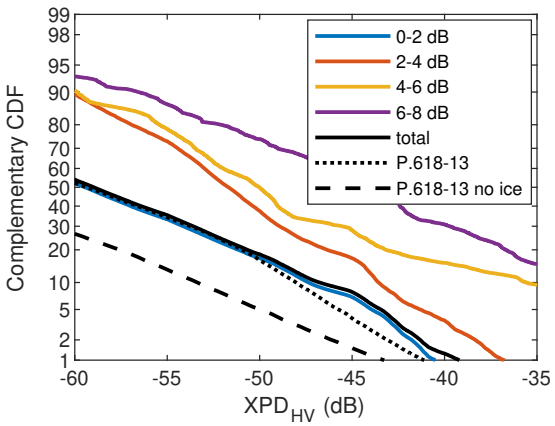

Figure 2. Gaussian integral chart of the XPD CCDFs at 18.7 GHz, not conditioned (black curve) and conditioned (coloured curves) to the selected CPA ranges. The dotted and dashed curves represent the ITU-R P.618-13 CCDF predictions, respectively including and neglecting the effect of the ice.

calculated and showed the 10, 50 and 90 percentiles of the data and the ITU-R P.618 model prediction of the equiprobable values of XPD and CPA. Mind that in this work we used the empirical CCDF of the data CPA as input of the ITU-R functional form. We can see that the mean and median values of the data substantially coincide. The majority of the data lay in a zone of attenuation lower than 5 dB,

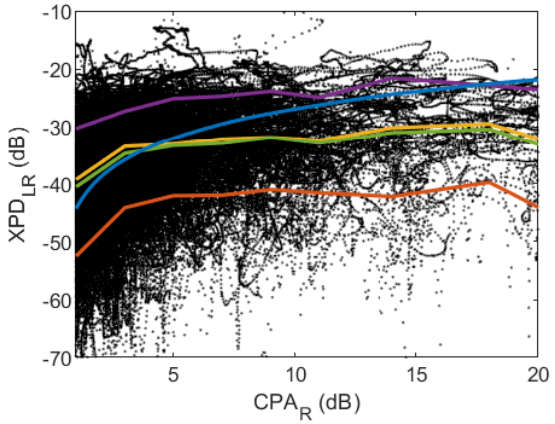

Figure 3. Scatterplot of XPD_{LR} and CPA_R, at 39.6 GHz. Red, yellow and purple curves are the 10, 50 and 90 percentiles of XPD conditioned to CPA values. The green curve is the mean. The cyan curve is the ITU-R P.618-13 model prediction.

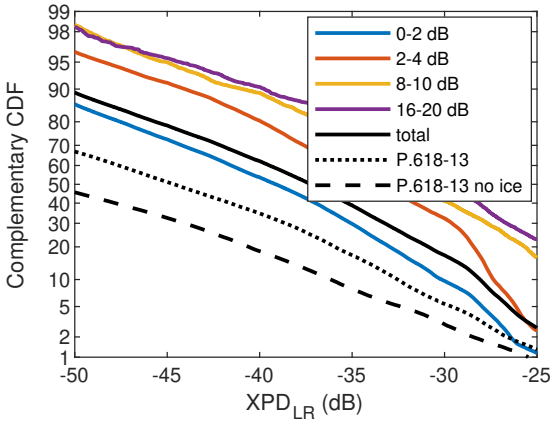

Figure 4. Gaussian integral chart of the XPD CCDFs at 39.6 GHz, not conditioned (black curve) and conditioned (coloured curves) to the selected CPA ranges. The dotted and dashed curves represent the ITU-R P.618-13 CCDF predictions, respectively including and neglecting the effect of the ice.

and we derived statistics up to 10 dB. Above this threshold the dataset is not statistically significant. Apart few outliers, the major part of the data are below a XPD value of about -30 dB. The prediction given by the functional form by ITU-R is close to the 90 percentile for excess attenuations lower than 5 dB and lays in a zone between the 90 and 50 percentiles for higher CPAs, which indicates that the ITU-R model of the equiprobable relationship between attenuation and depolarization of rain overestimates measurements also at higher attenuation values (larger than 5 dB). This can be due to the actual microphysical structure of rain (being less aligned and more turbulent than modelled) and to the combination of the effects of rain and ice particles along the path (which reduce the total XPD). On the other hand, we observe a relevant number of samples with high XPD (larger than -40 dB) for very low attenuation values (below 3 dB). This indicates a significant statistical effect of ice depolarization in absence of rain attenuation. In Figure 2 we showed the CCDF of the XPD at 18.7 GHz in a gaussian chart, conditioned to some CPA intervals. We have included the reference prediction by Recommendation P.618, both considering and neglecting the additional ice term. The irregular pattern of the curves conditioned to higher values of attenuation (i.e., 4-6 and 6-8 dB) is due to the low fraction of data represented at these CPA values. We can notice a fair accordance of the ITU-R prediction and the total CCDF up to a XPD value of -50 dB, beyond which the ITU-R model seems to underestimate the measured depolarization of few dB. With reference to the previous observation about the overestimation of the ITU-R model of rain depolarization, this indicates some effect of ice depolarization, in particular at low attenuation.

4.2 XPD statistics analysis at Q band

The XPD-CPA scatterplot is reported in Figure 3. In this case, the amount of data permits a statistical characterisation up to an attenuation of $15-20$ dB. It is interesting that,

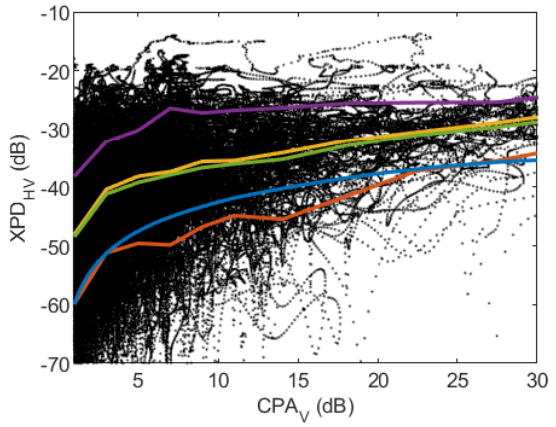

Figure 5. Scatterplot of XPD_{HV} and CPA_V, at 49.5 GHz. Red, yellow and purple curves are the 10, 50 and 90 percentiles of XPD conditioned to CPA values. The green curve is the mean. The cyan curve is the ITU-R P.618-13 model prediction.

being the signal circularly polarized (thus, not sensitive to the canting angle of atmospheric particles), the XPD levels reached are pretty high, up to -15 dB. Again, we included the mean and the 10, 50 and 90 percentiles of the data, as well as the functional form of the equipropable relationship between XPD and CPA of ITU-R P.618. At values of CPA lower than 5 dB, the ITU-R curve agrees with the median value of measurements. Then, as attenuation increases, it tends to the values corresponding to the 90 percentile. As in the Ka band case, this indicates that the ITU-R model can overestimate rain depolarization in presence of strong attenuation, and this could be due to a different microphysical structure of rain and the combination of rain and ice particles depolarization. The conditioning values of CPA were considered up to 20 dB also in the CCDF graph (Figure 4). When comparing this graph with the one for 18.7 GHz (Figure 2), we see that the measurements indicate a consistent underestimation (about 5 dB) of the ITU-R method for

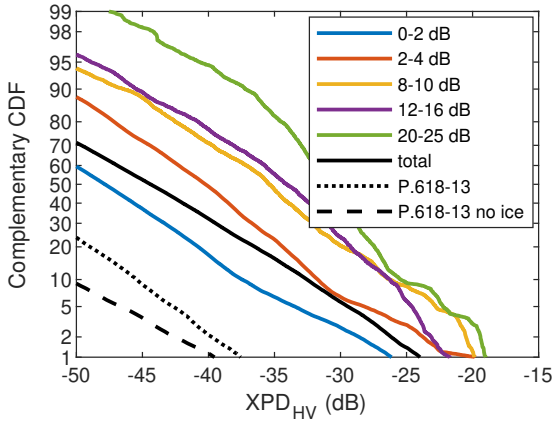

Figure 6. Gaussian integral chart of the XPD CCDFs at 49.5 GHz, not conditioned (black curve) and conditioned (coloured curves) to the selected CPA ranges. The dotted and dashed curves represent the ITU-R P.618-13 CCDF predictions, respectively including and neglecting the effect of the ice.

all the percentages of time. Considering that the equiprobable relationship of ITU-R for rain depolarization appears to agree or overestimate measurements, this can be ascribed to the effect of ice depolarization. The CPA-conditioned CCDFs are close to straight lines up to −30 dB of XPD, indicating the applicability of a normal distribution model.

4.3 XPD statistics analysis at V band

Last, we performed the analysis at 49.5 GHz. We chose to present here the XPD coming from the vertically polarized transmitted beacon, as in 4.1 (see Figure 5). Apart from few cases, the maximum value of XPD is lower than -20 dB, and we observe that the median and mean value of the measurements are very close. At this frequency, we observed that the ITU-R model for the equiprobable relationship between attenuation and depolarization of rain underestimates measured data, and actually corresponds to the lower percentiles of the observations (approximately between 30 and 10). This somehow differs from what observed at Ka and Q band, but it indicates an increased level of of ice depolarization at V band even in presence of intense rain. In Figure 6, we have the comparison of the CCDFs, for different CPA conditioning values. Again, as in Q band, we see that the lower amount of samples for higher attenuation affects the XPD distribution (see curves for attenuation 8 to 25 dB and XPD higher than -25 dB). However, for lower attenuations measurements, it can be described using a normal distribution. As at lower frequencies, the ITU-R model underestimates the values of measured XPD (up to 12 dB), and the use of the ITU-R ice correction factor does not have any major impact.

5 Conclusion

We analysed the atmospheric depolarization for SatCom systems operating at Ka, Q and V bands using experimental data collected at the Pomezia station with the ITALSAT satellite. We described the procedures adopted to remove the bias from the data. We showed the cumulative statistics of the measured atmospheric XPD − the main parameter quantifying depolarization in the transmission of EM waves due to atmospheric particles like raindrops and ice crystals − and its joint distribution with rain attenuation. We compared measurements with the current ITU-R P.618 Recommendation model prediction, to have a clear reference on the presented data. By comparing this model with the data for both the joint XPD-CPA and XPD distributions, we observed a varying level of agreement, depending on the frequency and the type of polarization. We may explain this behaviour to be a consequence of the microphysical modelling underneath the ITU-R functional form and the increase of relevance of ice on the total depolarization when moving from Ka to V band. We saw that, when representing a large fraction of data, the CCDFs could be modeled as a normal distribution. At the same time, we noticed a growing underestimation of the ITU-R P.618 model for the XPD CCDF with respect to the measured data, when frequency increases. The statistics presented in this article represent the basis on which building future XPD prediction models.

References

[1] J. Farserotu and R. Prasad, "A survey of future broadband multimedia satellite systems, issues and trends," *IEEE Communications Magazine*, **38**, 6, 2000, pp. 128–133, doi:10.1109/35.846084.

[2] T. Oguchi, "Electromagnetic wave propagation and scattering in rain and other hydrometeors," *Proceedings of the IEEE*, **71**, 9, 1983, pp. 1029–1078, doi:10.1109/PROC.1983.12724.

[3] Agenzia Spaziale Italiana, "ITALSAT Propagation Experiment: Users' Guide," *Telespazio*, 1992.

[4] A. Paraboni, A. Martellucci, C. Capsoni and C. G. Riva, "The physical basis of atmospheric depolarization in slant paths in the V band: theory, Italsat experiment and models," *IEEE Transactions on Antennas and Propagation*, **59**, 11, August 2011, pp. 4301–4314, doi:10.1109/TAP.2011.2164207.

[5] International Telecommunication Union, "Propagation data and prediction methods required for the design of Earth-space telecommunication systems, ITU Rec. ITU-R P.618-13," *ITU*, 2017.

[6] E. Matricciani, M. Mauri and C. Riva, "Relationship between scintillation and rain attenuation at 19.77 GHz," *Radio Science*, **31**, 02, 1996, pp. 273–279, doi:10.1029/95RS03475.

[7] P.H.G. van de Berg, G. Brussaard and J. Dijk, "On the accuracy of radiowave propagation measurements," *20th European Microwave Conference*, 1990, pp.656–661, doi:10.1109/EUMA.1990.336117.